Available online at www.sciencedirect.com

ScienceDirect

Procedia Structural Integrity 82 (2026) 153–161

Structural Integrity Procedia

www.elsevier.com/locate/procedia

8th International Conference on Structural Integrity and Durability (ICSID2025)

Ultrasonic Fatigue Behaviour of Additively Manufactured Ti-6Al-4V and Inconel 718: Influence of Build Orientation

D. Montalvão[a,*], S. Safari[b], P. Sewell[a], A. Abdelkader[a], R. Baxter[c], I. Johnston[c], D. McCluskey[c]

[a]*Bournemouth University, Poole House, Talbot Campus, Fern Barrow, Poole BH12 5BB, United Kingdom*
[b]*University of Bristol, Queens Building, University Walk, Clifton Campus, Bristol BS8 1TR, United Kingdom*
[c]*University of Hertfordshire, College Lane Campus, Hatfield AL10 9AB, United Kingdom*

Abstract

This study investigates build orientation effects on ultrasonic fatigue testing (UFT) calibration and mechanical behaviour of additively manufactured Ti-6Al-4V and Inconel 718 specimens. A statistical framework quantifies uncertainty propagation from measurement systems through calibration to stress-life estimation, which variability is a result from Additive Manufacturing (AM) specific variability including anisotropy, surface texture, and microstructural heterogeneity. Five specimens per material-orientation combination were tested at 20 kHz using Digital Image Correlation (DIC) and laser displacement measurements. Probabilistic calibration curves revealed orientation-dependent differences of 5-9% in stress-displacement relationships, with horizontal builds exhibiting higher effective stiffness than vertical builds. Monte Carlo simulations demonstrated that ±12.5% calibration uncertainty may propagate to two-order-of-magnitude variations (10^6 to 10^8 cycles) in predicted very high cycle fatigue (VHCF) life. Early fracture analysis identified build defects as dominant failure mechanisms. The framework provides confidence intervals essential for reliable VHCF characterization and industrial qualification of AM components in fatigue-critical applications.

Keywords: Ultrasonic fatigue testing; Additive manufacturing; Anisotropy; Uncertainty quantification; Digital Image Correlation

* Corresponding author. Tel.: +44 (0) 1202 965 513.
E-mail address: dmontalvao@bournemouth.ac.uk

10.1016/j.prostr.2026.04.024

1. Introduction

Additive manufacturing (AM) has revolutionised high-technology sectors such as aerospace, biomedical, and energy by enabling the fabrication of geometrically complex and lightweight components that were previously unachievable through conventional methods. As highlighted by Lopes et al. (2024), AM has transitioned from a prototype-focused to a product-dominant technology, driving innovation across multiple industries through enhanced design freedom, resource efficiency, and the ability to tailor material properties at the microstructural level. However, the layer-by-layer fabrication process introduces microstructural anisotropy, surface roughness, and stochastic defect populations that significantly influence mechanical properties, particularly fatigue performance (Yadollahi and Shamsaei, 2017). Understanding fatigue behaviour in the very high cycle fatigue (VHCF) regime (commonly defined as lifetimes beyond 10^7 cycles) is critical for structural integrity assessment (Bathias, 1999; Lopes et al., 2024), yet remains challenging due to the time-intensive nature of conventional fatigue testing and the inherent variability in AM materials (Bathias, 1999; Yadollahi and Shamsaei, 2017; Lopes et al., 2024)

UFT operating at approximately 20 kHz accelerates VHCF characterisation by three orders of magnitude compared to conventional servo-hydraulic testing at 10-400 Hz, reducing test durations from months to days (da Costa et al., 2020). However, UFT brings distinct calibration and uncertainty-quantification challenges: confidence intervals can be wider than with conventional, yet slower, servo-hydraulic tests, an effect exacerbated in the VHCF regime where dispersion and shallow S–N slopes make parameter estimation more sensitive (Safari et al., 2025). Besides, uncertainty becomes amplified when testing AM materials due to orientation-dependent properties, surface-texture effects on measurements, build defects such as voids, and spatially varying mechanical properties (Hong et al., 2023; Liu et al., 2024).

Recent literature demonstrates that build orientation fundamentally affects the performance of AM components. Ghadimi et al. (2023) showed that layer orientation influences high-frequency bending-fatigue life in 17-4 PH stainless steel by up to ≈40 %, with specimens loaded parallel to the build layers exhibiting superior performance. Lopes et al. (2024) comprehensively reviewed VHCF behaviour of additively manufactured metals, reporting fatigue-strength reductions of 30–50 % compared with wrought equivalents due to surface roughness (Ra = 5–15 μm, typical for as-built L-PBF), subsurface porosity (0.1–1 % volume fraction), and lack-of-fusion defects. These microstructural heterogeneities generate non-uniform stress fields that challenge conventional calibration assumptions.

The statistical treatment of UFT calibration uncertainty has recently been advanced through hierarchical Bayesian methods. Safari et al. (2025) developed a framework for conventional materials (EN8 steel) that quantifies measurement system uncertainties, machine dynamics variability, and specimen-to-specimen scatter, propagating these through to probabilistic stress-life curves. The hierarchical approach is particularly powerful because it learns parameters at multiple levels: individual specimen variability, population-level hyperparameters, and prediction uncertainty. However, this methodology has not been extended to AM materials, where additional complexity arises from orientation-dependent anisotropy, build-to-build variability, and defect-driven scatter.

This study addresses the need for systematic characterisation of orientation effects in UFT of AM materials. The specific objectives are to: (i) quantify orientation-dependent mechanical behaviour through combined DIC-laser measurements; (ii) establish calibration curves for both horizontal and vertical build orientations; (iii) assess calibration uncertainty and its implications; and (iv) investigate build defect influence on relative deformation performance.

2. Materials and Experimental methods

2.1. Materials and Specimen Fabrication

Ti-6Al-4V (Grade 5) and Inconel 718 specimens were manufactured using Laser Powder Bed Fusion (L-PBF) by 3T-AM in Newbury, UK. Two build orientations were investigated: horizontal (H), where the specimen longitudinal axis aligned with the build direction (Z-axis), and vertical (V), where the specimen axis was perpendicular to the build direction in the XY plane. This orientation choice creates fundamentally different loading conditions: in

vertical specimens, cyclic stress acts perpendicular to most layer interfaces, while in horizontal specimens, stress acts parallel to layer interfaces.

Five specimens of each material-orientation combination were produced in a single build to minimize batch-to-batch variability, yielding 20 specimens total (5x Ti-6Al-4V-V, 5x Ti-6Al-4V-H, 5x Inconel 718-V, 5x Inconel 718-H). The hourglass specimen geometry featured a diameter of 3.0 mm at the gauge section with transition radii designed to achieve first longitudinal natural frequency of approximately 20 kHz while maintaining uniform stress distribution in the gauge region. Specimens were machined to achieve close to mirror-finish surface texture (Ra ≈ 0.2 μm) at the gauge section (see Fig. 1).

Resonant frequencies measured for the assembled test system were 20,350±5 Hz for Inconel 718-H, 20,385±13 Hz for Inconel 718-V, 20,312±4 Hz for Ti-6Al-4V (H), and 20,291±9 Hz for Ti-6Al-4V (V).

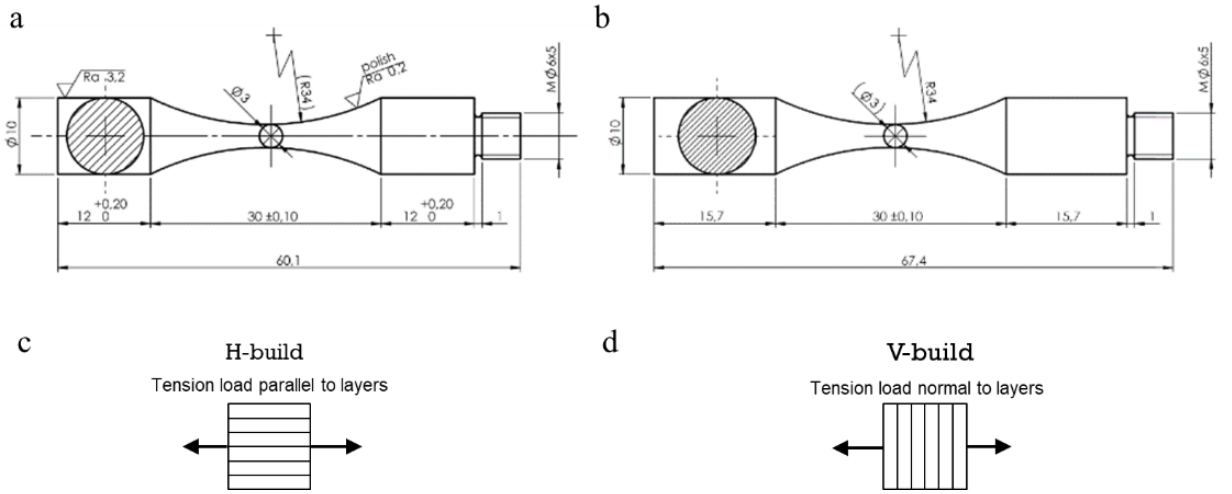

Fig. 1. (a) Geometry and dimensions of the ultrasonic fatigue testing specimen fabricated from Inconel 718; (b) geometry and dimensions of the Ti-6Al-4V (Ti64) specimen. (c) and (d) schematically represent the respective build orientations of the additively manufactured samples.

2.2. Ultrasonic fatigue testing system and measurement instrumentation

The UFT system at the ADDISONIC Research Cluster at Bournemouth University (Fig. 2) operates at 20 kHz and comprises: (i) piezoelectric transducer (1,250 W capacity, supplied by Branson); (ii) titanium alloy booster with 1:2 amplification ratio; (iii) EN19 steel custom-made tapered horn with 1:2 amplification ratio; (iv) specimen. The complete assembly resonates at its first longitudinal natural frequency, inducing purely axial cyclic loading.

Tip displacement was monitored using a Keyence LK-H027 ultra-high-speed laser displacement sensor with specifications: repeatability 0.02 μm, linearity ±0.05%, measurement range ±2.5 mm. Strain measurement employed a Dantec Dynamics Q-450 high-speed camera with Sigma 105 mm f/2.8 macro lens, providing spatial resolution of approximately 12 μm/pixel. For UFT calibration measurements, image acquisition was performed at 40 kHz with Digital Image Correlation (DIC) analysis using Istra4D software.

Temperature control was achieved through compressed air cooling using an intermittent testing protocol: vibration periods of 0.2-0.5 seconds alternating with rest periods, maintaining specimen temperature below 30°C as recommended by WES 1112:2022 standard (Furuya et al., 2022).

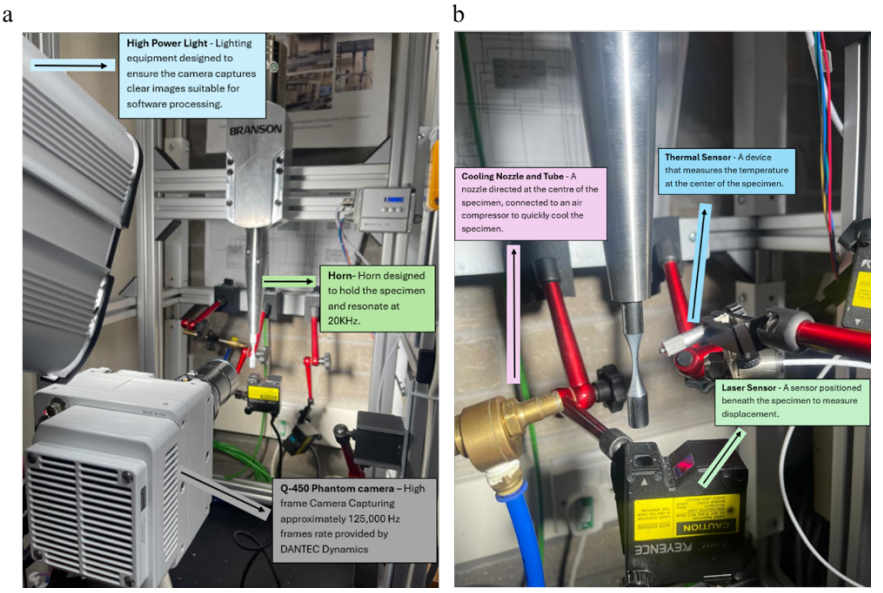

Fig. 2. Experimental UFT setup. (a) Overview of the 20 kHz stack showing the Branson horn, high-power illumination, and Q-450 Phantom high-speed camera. (b) Close-up view of the measurement and control instruments, including the cooling vortex tube, thermal sensor, and laser sensor for displacement measurement (Safari et al., 2024).

2.3. Calibration Procedure

For each specimen, the relationship between maximum principal strain at gauge center and tip displacement amplitude (Fig. 3) was characterised through systematic measurement. Simultaneous laser and DIC measurements were acquired at three displacement amplitudes (10, 12.5, 15 µm) spanning the operational range. This provided multiple data points per specimen for establishing the linear calibration relationship:

$$\sigma = \theta \cdot U \tag{1}$$

where σ is stress at gauge center (MPa), U is tip displacement (μm), and θ is the calibration parameter ($MPa/\mu m^{-1}$).

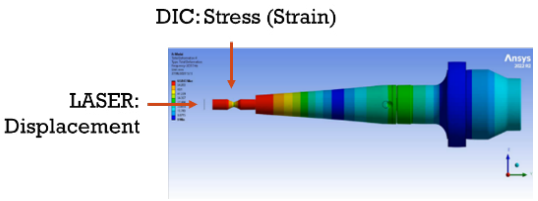

Fig. 3. Finite element model of the horn–specimen assembly showing the longitudinal vibration mode at 20 kHz, with arrows indicating the DIC and laser sensor measurement locations.

3. Results

3.1. Calibration Results: Inconel 718

Fig. 4 shows the calibration curve for Inconel 718, including 95% confidence interval and prediction bands from Monte Carlo simulations. The calibration parameters obtained from experimental measurements were:

- Inconel 718 - Horizontal: $24.66 \pm 1.20\ MPa/\mu m$ ($R^2 = 0.989, CV = 4.88\%$)
- Inconel 718 - Vertical: $23.43 \pm 1.25\ MPa/\mu m$ ($R^2 = 0.999, CV = 5.33\%$)

This represents a 5.2% difference in calibration slope between orientations. Horizontal specimens exhibited higher calibration parameter, meaning the same tip displacement produces greater stress at the gauge section. This observation indicates that horizontal specimens have effectively higher stiffness along the loading axis.

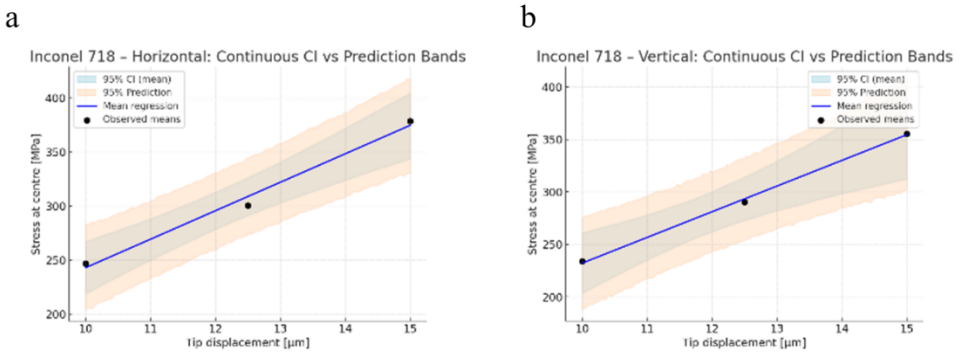

Fig. 4. Monte Carlo–based regression of stress at the specimens' centre *vs* tip displacement for Inconel 718: (a) horizontal build and (b) vertical build. Shaded regions indicate the 95 % confidence interval (blue) and 95 % prediction band (orange) derived from simulated distributions.

3.2. Calibration Results: Ti-6Al-4V

Fig. 5 shows the calibration curve for Ti-6Al-4V, including 95% confidence interval and prediction bands from Monte Carlo simulations. The calibration parameters obtained from experimental measurements were:

- Inconel 718 - Horizontal: $14.33 \pm 0.46\ MPa/\mu m$ ($R^2 = 0.997, CV = 3.21\%$)
- Inconel 718 - Vertical: $13.32 \pm 0.70\ MPa/\mu m$ ($R^2 = 0.998, CV = 5.24\%$)

This represents a 7.6% difference in calibration slope between orientations, showing more pronounced anisotropy than Inconel 718. Horizontal build orientation again produces higher stress at the gauge center for the same tip displacement. Ti-6Al-4V horizontal orientation exhibited the lowest coefficient of variation (3.21%), indicating the most consistent calibration behavior.

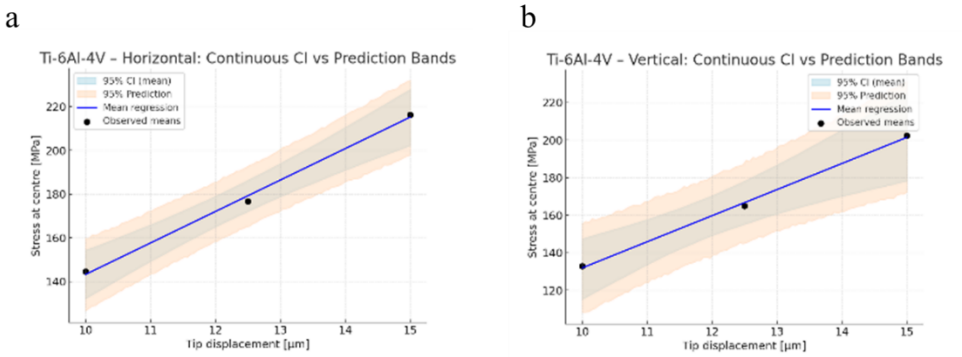

Fig. 5. Monte Carlo–based regression of stress at the specimens' centre *vs* tip displacement for Ti-6Al-4V: (a) horizontal build and (b) vertical build. Shaded regions indicate the 95 % confidence interval (blue) and 95 % prediction band (orange) derived from simulated distributions.

3.3. Anisotropy Comparison

Both materials show consistent anisotropy: horizontal orientation produces 5-8% higher calibration parameters than vertical orientation, indicating higher effective stiffness along the loading axis. Fig. 6 visually confirms this behaviour, with horizontal regression lines (red) consistently above vertical lines (blue) for both materials. Strain-displacement slopes differ by 6-9% between orientations (Inconel 718: $\varepsilon = 1.24 \times 10^{-4}$ vs $1.17 \times 10^{-4}\ \mu m^{-1}$; Ti-6Al-4V: $\varepsilon = 1.26 \times 10^{-4}$ vs $1.16 \times 10^{-4}\ \mu m^{-1}$).

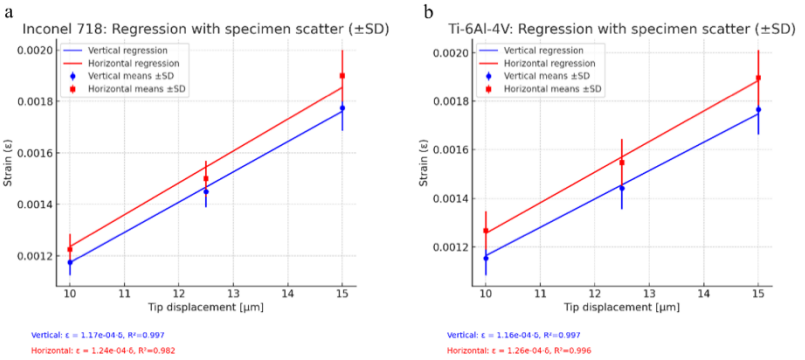

Fig. 6. Strain-displacement regression relationships for (a) Inconel 718 and (b) Ti-6Al-4V showing horizontal (red) and vertical (blue) orientations. Error bars represent ±SD across five specimens. All $R^2 > 0.98$.

Specimen-to-specimen variability was consistently higher for vertical orientation in both materials, visible as larger error bars in Fig. 6. This suggests greater sensitivity to build defects when loaded perpendicular to layers. The coefficient of variation ranged from 3.21% (Ti-6Al-4V horizontal) to 5.33% (Inconel 718 vertical).

All calibrations exhibited excellent linearity with $R^2 > 0.98$, confirming the stress-displacement relationship is well-characterised by a linear model across the tested range (10-15 μm).

3.4. Early Fracture Observation

One Ti-6Al-4V vertical specimen (V2) exhibited premature fracture during testing. According to test logs, this specimen broke after approximately 3.36 million cycles, with one-third of cycles at 10 μm displacement and two-thirds at 12.5 μm displacement. The specimen broke quickly when testing progressed to 15 μm displacement.

Optical microscopy of the fracture surface (Fig. 7) revealed visible defects that likely acted as crack initiation sites. This observation underscores that AM build defects can dominate fatigue behaviour in vertical orientation specimens where stress acts perpendicular to layer interfaces.

The fact that this early failure occurred in vertical orientation is consistent with the observation that vertical specimens show higher calibration variability, suggesting greater sensitivity to manufacturing defects when loaded perpendicular to build layers.

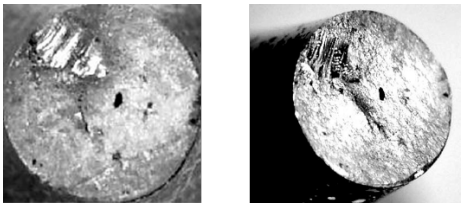

Fig. 7. Optical micrographs of Specimen Ti-6Al-4V after early failure at 15 μm displacement.

4. Discussion

4.1. Implications of Anisotropy for Component Design

The observed 5-8% difference in calibration parameters between horizontal and vertical orientations has direct implications for fatigue testing and component design. For fatigue-critical applications, horizontal build orientation provides higher effective stiffness and lower calibration variability. However, horizontal orientation may be geometrically infeasible or require support structures that compromise surface quality. Design optimisation must trade off orientation effects against manufacturing constraints.

The consistent finding that vertical orientation exhibits higher variability (30-40% higher coefficient of variation) indicates reduced predictability in fatigue performance. This suggests that when vertical orientation must be used, larger safety factors or more extensive testing may be warranted to account for the increased uncertainty.

4.2. Calibration Uncertainty and Testing Requirements

The excellent linearity ($R^2 > 0.98$) of all calibration curves confirms that the linear relationship given by equation (1) is appropriate for UFT calibration in the elastic regime. However, the specimen-to-specimen variability (CV = 3-5%) indicates that testing multiple specimens is essential for robust calibration, as already highlighted by Safari et al. (2025).

For reliable UFT characterisation of AM components, the following experimental design guidelines are recommended: (i) test both vertical and horizontal orientations to bound anisotropy effects; (ii) test a minimum of 5 specimens per material-orientation combination for adequate statistical characterisation; (iii) measure at 3-5 displacement levels spanning the operational range to confirm linearity; and (iv) account for the higher variability in vertical orientation when establishing test programs.

4.3. Monte Carlo Simulation and Uncertainty Propagation

Monte Carlo simulations were performed to visualise calibration uncertainty through confidence and prediction bands due to the reduced number of data points. As shown in Fig. 8, uncertainty can propagate to variations spanning from 10^6 to 10^8 cycles in predicted fatigue life. This two-order-of-magnitude range reflects the amplification of calibration uncertainty caused by the relatively shallow slope of the S–N curves in the VHCF regime.

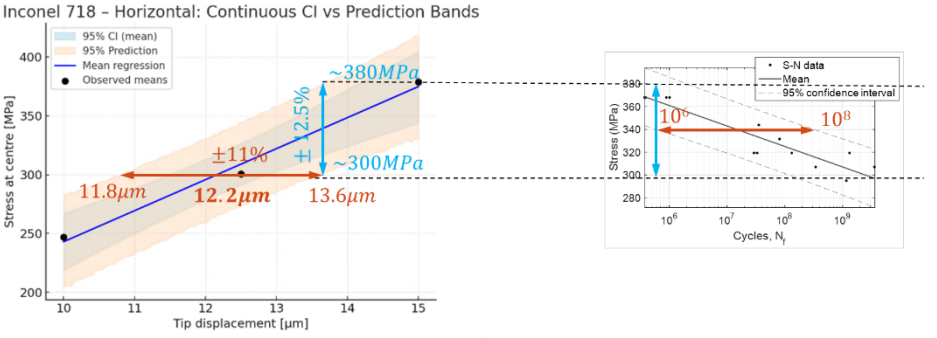

Fig. 8. Illustration of calibration-related uncertainty propagation in ultrasonic fatigue testing. (a) Monte Carlo regression for Inconel 718 (horizontal build) showing 95 % confidence and prediction bands, where displacement variation of ±2.5 % corresponds to stress differences of ~80 MPa. (b) Example S–N response highlighting that such stress variation can translate into a two-order-of-magnitude scatter in predicted fatigue life (10^6–10^8 cycles) due to the shallow slope typical of VHCF behaviour.

This finding emphasises that even with rigorous calibration procedures, AM material variability introduces unavoidable life prediction uncertainty. Conservative design approaches with appropriate safety factors are warranted when using UFT data for component qualification.

4.4. Comparison with Literature

The observed anisotropy magnitude (5-8% difference in calibration parameters between orientations) is consistent with orientation-dependent mechanical property variations reported for L-PBF Ti-6Al-4V materials (Leuders et al., 2013; Cain et al., 2015). The current results fall within ranges documented in the literature for similar AM processes, lending confidence to the measurement approach.

The early failure of Ti-6Al-4V-V2 is consistent with literature reports that AM materials exhibit increased defect sensitivity (Leuders et al., 2013; Gong et al., 2014), with defect-driven failures particularly pronounced when loading occurs perpendicular to build layers (Cain et al., 2015). Gong et al. (2014) documented that lack-of-fusion defects and gas porosity in the 50-150 μm size range can act as critical crack initiation sites in Ti-6Al-4V PBF components. This suggests that non-destructive evaluation such as computed tomography or high-resolution ultrasonic inspection (Tang et al., 2017) may be beneficial for fatigue-critical AM components to screen for defects above critical size thresholds before service.

4.5. Limitations

Several limitations warrant discussion: (i) Five specimens per condition is adequate for initial calibration characterisation but insufficient for full statistical confidence intervals. Larger sample sizes (n = 8-10) would reduce posterior uncertainty. (ii) All specimens came from one build batch, so build-to-build variability was not captured. Industry qualification requires testing across multiple builds and potentially multiple machines. (iii) The study focused on calibration rather than complete stress-life curves. Future work generating full S-N curves with runout samples is necessary to establish fatigue limits.

5. Conclusions and Future Work

This study characterised ultrasonic fatigue testing (UFT) calibration for additively manufactured Ti-6Al-4V and Inconel 718 specimens. The main findings are as follows:

- Anisotropy and variability: Build orientation significantly affects calibration, with 5–8 % differences in stress–displacement relationships (Inconel 718: 24.66 vs 23.43 MPa/μm; Ti-6Al-4V: 14.33 vs 13.32 MPa/μm). Vertical builds also showed 30–40 % higher scatter, reflecting greater defect sensitivity when loaded perpendicular to layers.
- Calibration linearity: All stress–displacement relationships were highly linear ($R^2 > 0.98$), confirming elastic-regime validity and consistency across materials and orientations.
- Defect influence: One Ti-6Al-4V vertical specimen failed prematurely (~3.36×10^6 cycles), with surface defects confirming the need for inspection and defect-control strategies.
- Practical guidance: UFT programmes should (i) test both orientations to capture anisotropy; (ii) use 5–10 specimens per condition; (iii) adjust safety factors for vertical builds; and, (iv) employ non-destructive evaluation for fatigue-critical components.

Further research should expand to complete S–N characterisation up to 10^9 cycles, enabling quantification of how ±5 % calibration uncertainty propagates through fatigue life predictions. Probabilistic Bayesian calibration methods (Safari et al., 2025) will be explored to capture anisotropy, defect, and microstructural variability. Integration of computed tomography for defect mapping, build-to-build variability assessment, and post-processing optimisation (surface finishing, heat and electromagnetic treatments, etc.) will support the development of defect-sensitive, reliability-based life-prediction models for industrial qualification of AM components.

Acknowledgements

The authors acknowledge Research England (United Kingdom) for financial support through the ADDISONIC Bournemouth University Strategic Investment Area. The authors also express their gratitude to 3T Additive Manufacturing Ltd. (https://www.3t-am.com/) for their in-kind contribution of test specimens, and in particular to Dr. Peter Jerrard for his technical support and collaboration in specimen preparation.

References

Bathias, C., 1999. There is no infinite fatigue life in metallic materials. Fatigue & Fracture of Engineering Materials & Structures 22, 559–565.

Cain, V., Thijs, L., Van Humbeeck, J., Van Hooreweder, B., Knutsen, R., 2015. Crack propagation and fracture toughness of Ti-6Al-4V alloy produced by selective laser melting. Additive Manufacturing 5, 68–76.

da Costa, P.R., Nwawe, R.T., Soares, H., Reis, L., Freitas, M., Chen, Y.K., Montalvão, D., 2020. Review of Multiaxial Testing for Very High Cycle Fatigue: From 'Conventional' to Ultrasonic Machines. Machines 8(2), 25.

Furuya, Y., Shimamura, Y., Takanashi, M., Ogawa, T., 2022. Standardization of an ultrasonic fatigue testing method in Japan. Fatigue & Fracture of Engineering Materials & Structures 45(8), 2415–2420.

Ghadimi, H., Jirandehi, A.P., Nemati, S., Ding, H., Garbie, A., Raush, J., Zeng, C., Guo, S., 2023. Effects of Printing Layer Orientation on the High-Frequency Bending-Fatigue Life and Tensile Strength of Additively Manufactured 17-4 PH Stainless Steel. Materials 16(2), 469.

Gong, H., Rafi, K., Gu, H., Starr, T., Stucker, B., 2014. Analysis of defect generation in Ti-6Al-4V parts made using powder bed fusion additive manufacturing processes. Additive Manufacturing 1–4, 87–98.

Fu, R., Zhenk, L., Zhong, Z., Hong, Y., 2023. High-cycle and very-high-cycle fatigue behavior at two stress ratios of Ti-6Al-4V manufactured via laser powder bed fusion with different surface states. Fatigue & Fracture of Engineering Materials & Structures 46, e13985.

Leuders, S., Thöne, M., Riemer, A., Niendorf, T., Tröster, T., Richard, H.A., Maier, H.J., 2013. On the mechanical behaviour of titanium alloy Ti-6Al-4V manufactured by selective laser melting: Fatigue resistance and crack growth performance. International Journal of Fatigue 48, 300–307.

Liu, H., Wang, L., Wang, H., Wang, J., Liu, Y., Zhang, J., Xie, L., 2024. Review on fatigue of additive manufactured metallic alloys: Microstructure, Performance, Enhancement, and Assessment Methods. Advanced Materials 36, 2306570.

Lopes, J.H., da Costa, P.R., Freitas, M., Reis, L., 2024. Review on the fatigue strength of additively manufactured metal materials under the very high cycle fatigue. Fatigue & Fracture of Engineering Materials & Structures 0, 1–22.

Safari, S., Montalvão, D., da Costa, P.R., Reis, L., Freitas, M., 2024. Calibration of an Ultrasonic Fatigue Testing Machine using Digital Image Correlation Technique. Presented at the 9th International Conference on Very High Cycle Fatigue (VHCF9), Lisbon, Portugal, 26–28 June 2024.

Safari, S., Montalvão, D., da Costa, P.R., Reis, L., Freitas, M., 2025. Statistical calibration of ultrasonic fatigue testing machine and probabilistic fatigue life estimation. International Journal of Fatigue 199, 109028.

Tang, M., Pistorius, P.C., Beuth, J.L., 2017. Prediction of lack-of-fusion porosity for powder bed fusion. Additive Manufacturing 14, 39–48.

Yadollahi, A., Shamsaei, N., 2017. Additive manufacturing of fatigue resistant materials: Challenges and opportunities. International Journal of Fatigue 98, 14–31.